PASJ: Publ. Astron. Soc. Japan , 1–??,

Helical Tomography of an Accretion Disk by Superhump Light Curves of the 2001 Outburst of WZ Sagittae

Yoji Osaki
Faculty of Education, Nagasaki University, Nagasaki, 852-8521
osaki@net.nagasaki-u.ac.jp

(Received 2003 April 2; accepted 2003 June 12)

Abstract

A new method for analyzing complex superhump light curves for the 2001 outburst of WZ Sagittae is proposed. The complexity arises because intrinsically time-varying and non-axisymmetric distributions of superhump light sources are coupled with the aspect effects around the binary orbital phase because of its high orbital inclination. The new method can disentangle these complexities by separating the non-axisymmetric spatial distribution in the disk from the time variation with the superhump period. It may be called a helical tomography of an accretion disk because it can reconstruct a series of disk images (i.e., disk's azimuthal structures) at different superhump phases. The power spectral data of superhump light curves of the 2001 outburst of WZ Sge by Patterson et al.(2002,PASP,114,721) are now interpreted under a new light based on the concept of helical tomography, and the azimuthal wave numbers of various frequency modes are identified. In particular, a frequency component, $n\omega_0 - \Omega$, where ω_0 and Ω are the orbital frequency and a low frequency of the apsidal precession of the eccentric disk, is understood as an $(n-1)$-armed traveling wave in the disk. A vigorous excitation of a wave component of $\cos(2\Theta - 3\omega_0 t)$ in the first week of the superhump era of WZ Sge, where Θ is the azimuthal angle, supports Lubow's (1991) theory of non-linear wave coupling of the eccentric Lindblad resonance for the superhump phenomenon. This method can in principle be applied to other SU UMa stars with high orbital inclination if light curves are fully covered over the beat cycle.

Key words: accretion, accretion disks — stars: binaries: close — stars: dwarf novae —stars: individual (WZ Sge) —stars: nova, cataclysmic variables

1. Introduction

WZ Sagittae, a prototype of one subclass of dwarf novae, called WZ Sge, underwent a full-scale outburst in 2001 July and extensive observations, particularly in optical light, covering almost all nights without any significant gaps, were made for more than one hundred days from the start of eruption on July 23 to the long fading to quiescence with a worldwide collaboration of amateur and professional astronomers. Its beautiful light curves can be found in VSNET (htpp://www.kusastro.kyoto-u.ac.jp/vsnet.DNe/wzsge01.html) and AAVSO, and some of them have already been published by Ishioka et al. (2002) and by Patterson et al (2002). The 2001 super-outburst of WZ Sge exhibited many interesting features, which will surely be discussed in the future by various workers. This paper addresses only one of those features, i.e., an analysis of complex light curves of common superhumps observed during the main outburst.

WZ Sge exhibited in its photometric light curves periodic humps repeating with a binary orbital period called either "outburst orbital humps" by Patterson et al (2002) or "early superhumps" by Ishioka et al (2002) or "early humps" by Osaki and Meyer (2002) for the first twelve days in its 2001 outburst. The origin of this phenomenon was discussed by Osaki and Meyer (2002) and by Kato (2002), and will not be discussed in this paper.

After the first twelve days, the common superhumps with a period of 1% longer than the binary orbit emerged in accordance with the SU UMa-type nature of WZ Sge stars. The superhumps then subsisted all the way to the end of the main outburst and during the so-called echo outbursts and in the long fading stage to quiescence (Patterson et al 2002), although they may be of "late superhump nature" in its later stage. The overall picture of the 2001 outburst of WZ Sge based on the disk instability model (i.e., the thermal–tidal instability model) was presented by Osaki and Meyer (2003) and may not need to be repeated here.

Once superhumps emerge, light curves of WZ Sge become extremely complex, as seen, e.g., in figure 5 of Patterson et al. (2002). Although they look extremely complex, one remarkable fact may be recognized, that is, the basic patterns of light curves were more or less repeated with the beat cycle of about six days between the superhump and the orbital periods. The reason why the superhump light curves in WZ Sge are so very complex is that intrinsically time-varying and non-axisymmetric distributions of superhump light sources are coupled with the aspect effects around the binary orbital phases because of its high orbital inclination (Osaki, Meyer 2003).

In this paper we propose a new method of light curve analysis to disentangle these complexities by separating the non-axisymmetric spatial distribution of the disk from

a time variation occurring with the superhump period. In section 2, we explain the basic concept of helical tomography and how to reconstruct an "orbital light curve" at a given superhump phase. In section 3, we present the inversion method of an "orbital light curve" at a given superhump phase into an azimuthal brightness distribution of the disk. In section 4 we interpret the power spectra of light curves in the common superhump era of the 2001 outburst of WZ Sge observed by Patterson et al. (2002) under a new light based on the concept of helical tomography, and we identify the azimuthal wave numbers of various frequency modes. In section 5 the modes observed in WZ Sge are interpreted in the context of Lubow's (1991) theory of non-linear wave interaction for the superhump phenomenon. Possible applications of the method to other cataclysmic variable stars are dealt with in section 6. Section 7 is a summary and discussions.

2. Basic Concept of Helical Tomography

It is now well established that the superhump phenomenon is produced by a tidally driven eccentric instability within accretion disks in cataclysmic variable stars (Whitehurst 1988; Hirose, Osaki 1990; Lubow 1991a,b). This instability occurs when an accretion disk expands to reach the 3:1 resonance region that excites the precessing eccentric structure in the accretion disk.

We first note that the superhump phenomenon is produced by the tidal stressing of a precessing eccentric disk by an orbiting secondary star, and that the intrinsic variation within the accretion disk is strictly periodic with the superhump period. We may see how light distributions in the disk of the superhump binary system vary with the superhump phase in hydrodynamic simulations [e. g., in figure 7b of Hirose and Osaki (1990), figure 8 of Murray (1998)]. In fact, observed superhump light variations in many SU UMa stars (those of low orbital inclination) are singly periodic. However, a complication arises when the superhump phenomenon occurs in cataclysmic variables with high orbital inclination because aspect effects cause other light variations in a non-axisymmetric disk, as shown by Simpson, Wood, and Burke (1998). These complications can be solved by the following method, which we call "helical tomography".

The method, itself, is very simple in principle. We reproduce at the first step an "orbital light curve" for a certain superhump phase, and then invert the "orbital light curve" thus obtained into brightness distribution in the disk for the given superhump phase. In this section we explain the method for reconstructing an "orbital light curve" for a given superhump phase. The inversion to an azimuthal brightness distribution in the disk is described in the next section.

In order to reconstruct an "orbital light curve" for a given superhump phase, we use all of the superhump light curves for one beat cycle of the orbital and superhump periods (i.e., about 6 days in the particular case of WZ Sge). Figure 1 illustrates the basic process of this method. Let us consider an ideal case in which superhump light

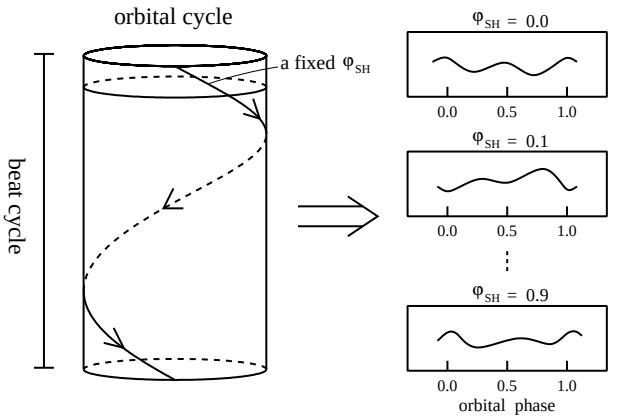

Fig. 1. Schematic illustrations showing how the helical tomography works. The cylinder in the left stands for light curve observations over one superhump beat cycle. The circle of the cylinder corresponds to one orbital cycle, while the beat phase proceeds from the top to the bottom of the cylinder. Let the number of orbital light curves in one beat cycle be N. The cylinder is then a sum of N thin cylinders. Each thin cylinder is thought to show one orbital light curve at a certain beat phase, although light curves are not shown here. In our helical tomography, we cut a small piece from each orbital light curve at a given superhump phase, $\varphi_{\rm SH}$, proceeding from the top to the bottom as illustrated by a helix in the left figure. We then assemble them into a fictitious "orbital light curve" at a given superhump phase as shown in the right figure. In this example we get ten "orbital light curves" for ten superhump phases. Each "orbital light curve" is then inverted to azimuthal light distribution for a given superhump phase by a method described in section 3. We call this method "helical tomography" because it can reconstruct a series of disk images (i.e., azimuthal light distribution) at different superhump phases, and because we cut out pieces of light curves "helically" to construct new light curves for certain superhump phases.

curves are completely covered over the superhump beat cycle, i.e., in the case of WZ Sge, with an orbital period of 0.05669 d and a superhump beat period of about 6 d, which results in about 100 orbital light curves. We then align these one hundred light curves with increasing superhump beat phase, just like figure 5 of Patterson et al. (2002). We then cut them into small pieces in which each piece corresponds to a certain superhump phase. For instance, let us consider to reproduce ten light curves for ten superhump phases, $\varphi_{\rm SH}$. We then cut out ten pieces from each light curve, assemble them for a certain superhump phase with increasing beat phase, and paste them as a function of the orbital phase to construct new light curves (in this case ten light curves).

Each newly formed light curve is a fictitious "orbital light curve" at a given superhump phase, and can be inverted into an azimuthal brightness distribution of the disk by a method described in the next section. This then gives a disk image at a given superhump phase seen from a particular inclination of the binary. The advantage of this method is that we can disentangle the geometrical effects of the azimuthal light distribution for a given superhump phase from the intrinsic time variation of the superhump,

itself. In other words, we translate the time variations of original light-curves into azimuthal light distributions at certain superhump phases. We call this method "helical tomography" of an accretion disk, because it can reconstruct a series of disk images (i.e., azimuthal light distributions) at different superhump phases. The "helical tomography" is a medical terminology by which a three-dimensional image of a human body is reconstructed. We use this medical terminology because the method can be used to reconstruct a series of disk images in different superhump phases. The adjective "helical" is used in another sense in that we cut out "helically" pieces of light curves to construct new light curves for certain superhump phases (see, figure 1).

3. Inversion of an "Orbital Light Curve" at a Given Superhump Phase into Azimuthal Brightness Distribution of the Disk

3.1. A Simple Model for Superhump Light Distribution

In order to extract information about the superhump light distribution in the accretion disk from an "orbital light curve" at a given superhump phase obtained by the method described in the preceding section, we need to make some simplifying assumption concerning the superhump light source. Radiation from the accretion disk of SU UMa-type dwarf novae during the common superhump era consists of two different types of radiation. One is radiation from the surface of the whole accretion disk produced by the ordinary viscous dissipation; the other is that from tidal dissipation near the disk edge. When we discuss superhump light curves, it is the common practice that we are interested only in time-varying component with a time-scale less than the orbital period and we remove from the analysis secular time variation with a time-scale longer than the orbital period. In such cases we assume that the time-varying part of the radiation is solely produced by the tidal dissipation of the eccentric precessing disk, and that radiation from the main part of the accretion disk due to the ordinary viscous dissipation contributes only to the constant background radiation in superhump light curves.

To extract information about the spatial distribution of superhump light at a given superhump phase from "orbital light curves", we need to make further assumptions. Since an orbital light curve includes only "one-dimensional" information, we can extract only one-dimensional information of the disk. Admittedly, the terminology "helical tomography" may be an over-statement in this sense because we are not able to reconstruct two-dimensional images of the disk. However, we keep using this terminology because we can reconstruct a series of the disk images with different superhump phases. We adopt a simplest model for radiation from the tidal dissipation in a given superhump phase. As discussed by Osaki and Meyer (2003), the tidal dissipation at a given superhump phase is non-axisymmetric in its pattern, and occurs near the disk rim in a region of about 1/10 width in the disk radius, i.e., almost the same size as the estimated half thickness of the disk at its rim. Thus, about one half of the superhump light may be expected to be radiated from the two horizontal disk surfaces and one half from the vertical disk rim. For binary systems with a high orbital inclination, radiation from the tidal dissipation comes mostly from the vertical disk rim; its relative importance of the disk rim to the horizontal disk surface is proportional to $\tan i$, where i is the orbital inclination. Furthermore, we assume for simplicity that the surface of the accretion disk is flat, so that radiation from the horizontal disk surface for a given superhump phase is independent of the orbital aspect. In other words, we may consider only superhump light from the vertical disk rim and we may regard radiation from the disk surface as the constant background light with the above-mentioned assumption when we discuss its aspect dependence around the binary orbit.

3.2. Forward Problem: Transformation of Spatial Distribution of the Superhump Light at a Given Superhump Phase into Orbital Light Curve

To proceed further, we need to make some more simplifying assumptions concerning the spatial distribution of the superhump light. We here assume that the disk rim is a circular cylindrical surface with radius R, and vertical width H, and that the superhump light distribution at the disk rim is now represented by $I = I(\theta)$, where I is specific intensity of radiation and θ is the azimuthal angle of a surface element of the vertical rim in the corotating frame of the binary, respectively. Here, the azimuthal angle θ is measured in the direction of the binary orbital motion in our convention. That is, all of non-axisymmetric effects of the superhump light are assumed to be represented by an azimuthal dependence of the intensity of radiation at the circular disk rim.

This assumption is admittedly very crude as the disk rim is not certainly circular, but is elongated during the superhump era. Here, we have restricted our attention only to the azimuthal distribution of the superhump light by neglecting all other effects. That is the reason why I have adopted the above-mentioned assumption. Because of this shortcoming, we must be careful not to over-interpret the obtained results.

We represent the direction to the observer by (i, θ_0), where i is the orbital inclination and θ_0 is the azimuthal angle to the observer in the corotating frame. We here take into account the limb-darkening effect of a surface element, which is written by

$$I = I_{\rm c}\frac{(1+\beta\cos\vartheta)}{1+\beta}, \tag{1}$$

where $I_{\rm c}$ is the intensity of radiation along the surface normal, ϑ is the angle between the surface normal and the direction to the observer, and β is the limb-darkening coefficient. The angle between the surface normal and the direction to the observer, ϑ, is expressed by

$$\cos\vartheta = \sin i \sin\theta', \tag{2}$$

where θ' is an azimuthal angle of a disk surface element in the observer's frame in which the origin is chosen to the

direction perpendicular to the observer. The azimuthal angles in these two frames are related to each other by

$$\theta' = \theta - \theta_0 + \frac{\pi}{2}. \tag{3}$$

Let us consider some certain superhump light distribution from the disk rim at a given superhump phase, which is represented by $I_{\rm c} = I_{\rm c}(\theta)$. We may expand it into its Fourier components as

$$I_{\rm c} = \sum_{m=0}^{m=\infty} I_m \cos(m\theta + \phi_m), \tag{4}$$

where $m = 0, 1, 2, 3, ...$ are zero and positive integers and ϕ_m is a constant phase for a given m.

In what follows, we discuss each of Fourier components separately. The radiation emitted to the observer from length $Rd\theta$ of the cylindrical surface is $RH\cos\vartheta I_m \cos(m\theta + \phi_m)d\theta$ for the m-th Fourier component. We now integrate the light contribution for the visible surface of the cylinder, for which θ' varies from 0 to π. The m-th component of radiation received by the observer will then be

$$F_m(\theta_0) = \frac{RHI_m/D^2}{1+\beta} \times \int_0^{\pi} (1+\beta\cos\vartheta)\cos\vartheta\cos(m\theta+\phi_m)d\theta', \tag{5}$$

where D is the distance of the observer from the star. Substituting equations (2) and (3) into equation (5), we obtain

$$F_m(\theta_0) = \frac{RHI_m/D^2}{1+\beta} \times \int_0^{\pi} (\sin i\sin\theta' + \beta\sin^2 i\sin^2\theta') \times \cos\left(m\theta' + m\theta_0 + \phi_m - \frac{m\pi}{2}\right) d\theta'. \tag{6}$$

After some elementary calculations, we can show that equation (6) can be written as

$$F_m(\theta_0) = \frac{RHI_m/D^2}{1+\beta}\sin i \times (A_m + \beta\sin iB_m)\cos(m\theta_0+\phi_m), \tag{7}$$

where A_m and B_m are numerical constants.

Equation (7) is the very equation which we have sought, and it tells us that the orbital light variation due to the m-th component of superhump light is proportional to the intensity at the very surface element of the disk rim facing to the observer, i.e., the surface element at the azimuthal angle θ_0. The coefficients A_m and B_m represents how much reduction of light occurs due to integration over the visible surface of the disk rim. As shown below, they decrease rapidly by going to the higher order m-mode because of cancellation effects with positive and negative light contributions.

It is found that the coefficient A_m is given for an even integer m by

Table 1. Coefficients A_m and B_m, and coefficient C_m for two cases with no limb darkening and with limb darkening of $\beta = 0.56$ and $i = 90°$.

m	A_m	B_m	C_m ($\beta = 0$)	C_m ($\beta = 0.56$)
0	2	$\pi/2$	1	0.923
1	$\pi/2$	4/3	0.785	0.743
2	2/3	$\pi/4$	0.333	0.355
3	0	4/15	0	0.048
4	-2/15	0	-0.067	-0.043
5	0	-4/105	0	-0.00068
6	2/35	0	0.029	0.018

$$A_m = (-1)^{1+m/2}\frac{2}{m^2-1}, \tag{8}$$

while $A_m = 0$ for odd integers m, except for $m = 1$. The case for $m = 1$ is an exception and $A_1 = \pi/2$. Similarly, the coefficient B_m is given for odd integers by

$$B_m = (-1)^{(m+1)/2}\frac{4}{m(m^2-4)}, \tag{9}$$

while $B_m = 0$ for even integer m, except for $m = 0$ and $m = 2$, for which $B_0 = \pi/2$ and $B_2 = \pi/4$. Equation (7) may be written in a more convenient form as

$$F_m(\theta_0) = \frac{2RH}{D^2}\sin iI_m C_m \cos(m\theta_0+\phi_m) \tag{10}$$

$$= F_m^0 \cos(m\theta_0 + \phi_m), \tag{11}$$

where the coefficient

$$C_m = \frac{A_m + \beta\sin iB_m}{2(1+\beta)} \tag{12}$$

is the transformation coefficient from the brightness distribution of the disk rim to the orbital light curve. It is normalized to one for a disk rim with uniform brightness and no limb darkening. Their numerical values are listed in table 1 for two cases with no limb darkening and with limb darkening of $\beta = 0.56$ and an inclination of $i = 90°$ together with coefficients A_m and B_m.

3.3. Inversion: Reconstruction of Azimuthal Brightness Distribution of the Disk from Orbital Light Curve

The inversion from the orbital light curve to the azimuthal brightness distribution is straightforward in our case. Let us write an orbital light curve as $F = F(\varphi_0)$ for a certain superhump phase obtained by the method described in section 2, where φ_0 is the orbital phase in angular units. The orbital phase φ_0 and the azimuthal angle of the observer in the corotating frame of the binary, θ_0, used in the previous subsection are related each other by $\varphi_0 = 2\pi - \theta_0$. Since $F = F(\varphi_0)$ is a periodic function with 2π, we may expand the orbital light curve into Fourier series as

$$F = \sum_{m=0}^{m=\infty} F_m^0 \cos(m\varphi_0 - \phi_m) \tag{13}$$

Table 2. Observed power spectra of superhump light curves in the first week of the common superhump era for the 2001 outburst of WZ Sge (data from Patterson et al 2002).

n	Frequency (c d^{-1})	Power	Relative amp. a_n	Identification
1	17.49	1030	32	$\omega_0 - \Omega$
2	17.64	~ 60	7.7	ω_0
3	34.97	~ 85	9.2	$2\omega_0 - 2\Omega$
4	35.12	~ 35	5.9	$2\omega_0 - \Omega$
5	52.77	~ 50	7.1	$3\omega_0 - \Omega$

$$= \sum_{m=0}^{m=\infty} F_m^0 \cos(m\theta_0 + \phi_m), \tag{14}$$

where F_m^0 is a Fourier amplitude with m-th component. Here ϕ_m is a constant phase of the m-th component and a minus sign is attached to ϕ_m in equation (13) because it has turned out that the constant phase ϕ_m defined in this subsection is identical to that defined in the preceding subsection. We note here that the zeroth component, F_0, includes not only contributions from the vertical disk rim, but also from the horizontal disk surface.

We now recover individual mode amplitudes, I_m, of the azimuthal brightness distribution of the disk by inverting equation (11) to obtain

$$I_m = \left(\frac{D^2}{2RH\sin i}\right)\frac{F_m^0}{C_m}. \tag{15}$$

Once we obtain all Fourier amplitudes, we reconstruct the disk image by adding all Fourier components in equation (4).

4. New Light on the Power Spectra of Superhump Light Curves for the 2001 Outburst of WZ Sge

Patterson et al. (2002) made a power spectral analysis of superhump light curves of the 2001 outburst of WZ Sge over the full beat cycle, and obtained many frequencies; all were linear combinations of ω_0 and Ω, where ω_0 and Ω are the orbital frequency and the putative apsidal frequency of an eccentric disk, respectively. As a matter of fact, we do not even need to construct new "orbital light curves" to demonstrate the power of the helical tomography if we already have information of power spectra of superhump light curves.

We explain this by using Patterson et al's (2002) data for the first week of the common superhump era of the 2001 outburst of WZ Sge. Table 2 summarizes results of power spectral analysis taken from their figure 6. Each column of table 2 indicates from left to right, the ordinal number, n, of individual modes with increasing frequency, cyclic frequency in units of cycle d^{-1}, power of modes estimated by eye from their figure 6, relative amplitudes of modes, a_n, and its identification. As can be seen in their figure 6, five discrete peaks in power spectra are seen and there is no ambiguity of their identification. Two largest peaks at $\omega_0 - \Omega = 17.49$ c d^{-1} and $2\omega_0 - 2\Omega = 34.97$ c d^{-1} are those of the superhump period and its first harmonics, corresponding to the superhump light curve shown by Patterson et al.(2002) at the lowest left frame of their figure 6, which was obtained by synchronous summation at the superhump period. The most interesting is the signal at $3\omega_0 - \Omega = 52.77$ c d^{-1} which appears as an isolated peak at the frequency range of the second harmonics and its side bands. As will be shown below, it is identified a traveling two-armed spiral wave.

The light intensity in the first week of the common superhump era is expressed as

$$\begin{aligned} &L(t) \\ &= L_0 + a_1\cos[(\omega_0-\Omega)t+\psi_1] + a_2\cos(\omega_0 t+\psi_2) \\ &\quad + a_3\cos[2(\omega_0-\Omega)t+\psi_3] + a_4\cos[(2\omega_0-\Omega)t+\psi_4] \\ &\quad + a_5\cos[(3\omega_0-\Omega)t+\psi_5], \end{aligned} \tag{16}$$

where L_0 stands for the background light and a_i and ψ_i are the amplitudes and constant phases for the respective modes. In equation (16) and following mathematical expressions, we understand that the frequencies, such as ω_0 and Ω, and phases, such as $\varphi_{\rm SH}$ and $\varphi_{\rm beat}$, are given in angular units because there may be no confusion, for instance, with cyclic frequencies. Equation (16) is rewritten for later convenience as

$$\begin{aligned} &L(t) \\ &= L_0 + a_1\cos[(\omega_0-\Omega)t+\psi_1] \\ &\quad + a_3\cos[2(\omega_0-\Omega)t+\psi_3] + a_2\cos(\omega_0 t+\psi_2) \\ &\quad + a_4\cos[\omega_0 t+(\omega_0-\Omega)t+\psi_4] \\ &\quad + a_5\cos[2\omega_0 t+(\omega_0-\Omega)t+\psi_5]. \end{aligned} \tag{17}$$

Let N denote the number of the orbital light curves in the beat cycle, which is given by the nearest integer of the ratio ω_0/Ω. A particular time in the n-th light curve is then expressed as

$$\omega_0 t = 2\pi(n-1) + \varphi_0, \tag{18}$$

$$(\omega_0-\Omega)t = 2\pi(n-1) + \varphi_{\rm SH}, \tag{19}$$

where φ_0 and $\varphi_{\rm SH}$ are the orbital phase and the superhump phase, respectively. They are related to each other by $\varphi_0 = \varphi_{\rm SH} + \varphi_{\rm beat}$, where $\varphi_{\rm beat} = \Omega t$ is the beat phase. Substituting equations (18) and (19) into equation (17), we obtain

$$\begin{aligned} L = L_0 &+ a_1\cos(\varphi_{\rm SH}+\psi_1) + a_3\cos(2\varphi_{\rm SH}+\psi_3) \\ &+ a_2\cos(\varphi_0+\psi_2) + a_4\cos(\varphi_0+\varphi_{\rm SH}+\psi_4) \\ &+ a_5\cos(2\varphi_0+\varphi_{\rm SH}+\psi_5). \end{aligned} \tag{20}$$

Let us now use the concept of helical tomography, in which each "orbital light curve" corresponds to a fictitious light curve of a snap shot of the accretion disk [see, e.g., ten snap shots of the accretion disk in figure 7 of Hirose and Osaki (1990)] viewed from different azimuthal directions. We may regard equation (20) as that describing an "orbital light curve" at a given superhump phase. That is, in the above equation $\varphi_{\rm SH}$ is regarded to be a fixed

constant, while $\varphi_0 = 2\pi - \theta_0$ is a variable orbital phase, representing the azimuthal angle of the line of sight of an observer in the co-rotating frame of the binary.

We may rewrite equation (20) as

$$L = L_0 + a_1\cos(\varphi_{\rm SH}+\psi_1) + a_3\cos(2\varphi_{\rm SH}+\psi_3) + a_2\cos(\theta_0-\psi_2) + a_4\cos(\theta_0-\varphi_{\rm SH}-\psi_4) + a_5\cos(2\theta_0-\varphi_{\rm SH}-\psi_5). \quad (21)$$

By using the method described in the preceding section, we now invert equation (21) to obtain the surface brightness distribution of the vertical disk rim as

$$I(\theta,\varphi_{\rm SH})\left(\frac{2RH\sin i}{D^2}\right) = L_0 + b_1\cos(\varphi_{\rm SH}+\psi_1) + b_3\cos(2\varphi_{\rm SH}+\psi_3) + b_2\cos(\theta-\psi_2) + b_4\cos(\theta-\varphi_{\rm SH}-\psi_4) + b_5\cos(2\theta-\varphi_{\rm SH}-\psi_5), \quad (22)$$

where $b_1 = a_1$, $b_3 = a_3$, $b_2 = a_2/C_1$, $b_4 = a_4/C_1$, and $b_5 = a_5/C_2$ in the case of no limb darkening.

Equation (22) represents the azimuthal brightness distribution of the superhump light at the disk rim for a given superhump phase. In order to reconstruct the brightness distribution of the disk for a certain superhump phase, we need information about the constant phases, ψ_n, of individual Fourier components. Unfortunately, this information is usually not available in published form. Since the phase information of individual modes has turned out to be very important from the standpoint of the helical tomography, we urge observers to publish such information together with the amplitudes of individual modes.

Since $\varphi_{\rm SH} = (\omega_0 - \Omega)t$, we may rewrite the above equation as

$$I(\theta,t)\left(\frac{2RH\sin i}{D^2}\right) = L_0 + b_1\cos[(\omega_0-\Omega)t+\psi_1] + b_3\cos[2(\omega_0-\Omega)t+\psi_3] + b_2\cos(\theta-\psi_2) + b_4\cos[\theta-(\omega_0-\Omega)t-\psi_4] + b_5\cos[2\theta-(\omega_0-\Omega)t-\psi_5]. \quad (23)$$

Equation (23) describes the brightness distribution of the superhump light as a function of the azimuthal angle, θ, in the disk and time, t. As expected, it is a periodic function with the superhump period.

The first line of the right hand side of equation (23) is then a certain constant at a given superhump phase, representing the light level of a synchronously summed superhump light curve (see, the lowest left panel of figure 6 of Patterson et al. 2002). The second line of equation (23) represents a one-armed wave fixed in the corotating frame of the binary. It corresponds to the lowest right panel of the same figure; however a much clearer figure is found in the lowest right panel of figure 7 for the second week of the common superhump era (Patterson et al. 2002). This was called "mean orbital light curve", and was interpreted as a hot spot light curve by Patterson et al. (2002). As discussed by Osaki and Meyer (2003), we have argued that the "mean orbital light curve" simply represents the non-axisymmetric distribution of the superhump light, and that it is not due to the enhanced hot spot. This point will be taken up once more in the next section.

The third line also represents a one-armed wave, but this time it is a traveling wave which rotates progradely once per superhump period in the co-rotating frame, because

$$\frac{d\theta}{dt} = \omega_0 - \Omega. \quad (24)$$

If we introduce the azimuthal angle in the inertial frame by Θ, it is related to that in the corotating frame by $\Theta = \theta + \omega_0 t$. Thus, this wave mode rotates twice in the inertial frame per superhump period.

From the same discussion as given above, we find that the last term of the right-hand side represents a two-armed traveling wave, as

$$\frac{d\theta}{dt} = \frac{\omega_0 - \Omega}{2}. \quad (25)$$

That is, the wave pattern rotates one half per superhump period in the corotating frame. However, the same disk configuration returns back after one superhump period because the basic pattern is two-armed.

The brightness distribution of the disk can also be expressed in the inertial frame (i.e., in the observer's frame). Since the azimuthal angle in the inertial frame, Θ, is related to that in the corotating frame, θ, by $\theta = \Theta - \omega_0 t$, equation (23) is rewritten as

$$I(\Theta,t)\left(\frac{2RH\sin i}{D^2}\right) = L_0 + b_1\cos[-(\omega_0-\Omega)t-\psi_1] + b_3\cos[-2(\omega_0-\Omega)t-\psi_3] + b_2\cos(\Theta-\omega_0 t-\psi_2) + b_4\cos[\Theta-(2\omega_0-\Omega)t-\psi_4] + b_5\cos[2\Theta-(3\omega_0-\Omega)t-\psi_5]. \quad (26)$$

Equation (26) describes the brightness distribution of the disk in the inertial frame.

The above results are summarized in table 3 where wave modes are specified by (m,ℓ) in which the brightness distribution in the disk is written as $\cos(m\Theta - \ell\omega_0 t)$. Here, a small frequency shift of Ω to $\ell\omega_0$ is disregarded in specifying the wave modes, because $\Omega \ll \omega_0$. The mode identification of five modes with (m,ℓ) is straight forward from equation (26). The main peak of the power spectrum (i.e., the $n = 1$ mode) is the well-known superhump periodicity with frequency $\omega_0 - \Omega$ and its wave is identified by the $(0,1)$-mode because there is no dependence on the azimuthal angle, Θ, as seen from equation (26). The slowly precessing eccentric disk mode with $\cos(\Theta - \Omega t)$-wave is identified as the $(1,0)$-mode but this mode, itself, does not produce any brightness distribution except for secular variation with the beat period (i.e., $2\pi/\Omega$). The tidal coupling of the eccentric $(1,0)$-mode with the companion's gravitational field described by (m,m)-waves produces $(m-1,m)$-modes as discussed in Lubow (1991a) and in the next section. The superhump light variation

Table 3. Mode identifications and inverted amplitudes of individual modes.

n	Frequency (c d^{-1})	Identification	Mode (m,ℓ)	Inverted amp. b_n
1	17.49	$\omega_0-\Omega$	(0,1)	32
2	17.64	ω_0	(1,1)	9.8
3	34.97	$2\omega_0-2\Omega$	(0,2)	9.2
4	35.12	$2\omega_0-\Omega$	(1,2)	7.5
5	52.77	$3\omega_0-\Omega$	(2,3)	22

with the $(0,1)$-mode is produced by a tidal interaction between the eccentric $(1,0)$-mode and the tidal $(1,1)$-mode. The various wave modes excited in the superhump disk are discussed in the next section.

We find from table 3 that the wave mode with $\cos(2\Theta-3\omega_0 t)$ was very strongly excited in the first week of the common superhump era in the 2001 outburst of WZ Sge; its significance is discussed in the next section.

The above result can easily be extended to a Fourier component with frequency $n\omega_0-\Omega$. Since the time dependence of this mode is written as

$$\cos[(n\omega_0-\Omega)t+\psi_n]=\cos[(n-1)\varphi_0+\varphi_{\rm SH}+\psi_n)]\,, \quad (27)$$

it represents an $(n-1)$-armed traveling wave which rotates $[1/(n-1)]$-times per superhump period. However, the basic disk configuration returns back after one superhump period because of its $(n-1)$-armed structure. Patterson et al. (2002) found in the second week of the common superhump era of the 2001 outburst of WZ Sge the primary Fourier components at $n\omega_0-\Omega$ in the power spectrum with $n=1,2,3,4,5,6,7,8,9$. These are exactly $(n-1)$-armed waves discussed here. The appearance of higher Fourier components in the second week indicates the appearance of a much shaper feature in the second week for the azimuthal brightness distribution in the disk.

5. Lubow's Theory of Non-Linear Wave Coupling by the Eccentric Lindblad Resonance

In the previous section we have demonstrated that by using the concept of helical tomography we can identify azimuthal wave numbers of various frequencies found in the power spectral analysis of superhump light curves by Patterson et al (2002). In particular, we identify the Fourier components at $n\omega_0-\Omega$ as $(n-1)$-armed traveling waves. In this section, we discuss why these wave modes are excited in the accretion disk of a superhump binary. To do so, we use Lubow's theory (1991a,b) of non-linear wave coupling. Below, we basically follow Lubow's (1991a,b) discussions on this problem.

In this section, we use mostly the inertial frame of reference rather than the corotating frame. The tidal perturbing potential in the accretion disk by the secondary star is expressed as

$$\phi(r,\Theta)=\phi_m(r)\cos(m\theta)=\phi_m(r)\cos\left[m(\Theta-\omega_0 t)\right]. \quad (28)$$

Let us consider wave fields in the accretion disk which are specified by two integers (m,ℓ) in which its azimuthal and time dependence is expressed as $\cos(m\Theta-\ell\omega_0 t)$. The tidal perturbation potential produces forced wave fields with $m=m$ and $\ell=m$, as is known very well.

Let us now impose some finite eccentricity in the accretion disk. The disk eccentricity is described as a one-armed eigenmode whose eigenfrequency, Ω, is known to be very small as compared with ω_0 (see, Hirose, Osaki 1993). Following Lubow (1991a), we denote this mode as the (1,0)-mode. The non-linear wave coupling between the $(1,0)$-mode and the (m,m)-mode produces another wave mode with $(m-1,m)$. Lubow (1991a,b) has demonstrated that, in particular, a strong wave with $(2,3)$ is launched at the 3:1 resonance region of the accretion disk by the eccentric Lindblad resonance. Further coupling between the $(m-1,m)$-mode and the (m,m)-mode reinforces the imposed eccentric mode with (1,0). This is Lubow's picture of excitation of the eccentric mode by the eccentric Lindblad resonance.

So far we have neglected the small, but finite, frequency, Ω, of the eccentric mode to describe various (m,ℓ)-modes. Let us now take into account slow precession of an eccentric mode (1,0). This mode has a small, but finite, frequency of Ω, describing a beat period of about 6 days in the case of WZ Sge. Since the $(m-1,m)$-mode is produced by coupling between the (1,0)-mode and the (m,m)-mode, its frequency is given by $m\omega_0-\Omega$. This is exactly the $(m-1)$-armed traveling wave discussed in the previous section.

The $(0,1)$-mode with frequency $\omega_0-\Omega$ corresponds to the main peak of the power spectrum of the common superhump era with the superhump period, only a periodicity to be observed in superhump binary systems with a low orbital inclination. Many peaks in the power spectra found by Patterson et al (2002) in the common superhump era are those with $m\omega_0-\Omega$, which are interpreted as the $(m-1,m)$ mode in the previous section. The dominance of these modes in the common superhump era is a natural consequence of Lubow's (1991) theory. In particular, the fact that the $(2,3)$ mode at a frequency $3\omega_0-\Omega$ is very strong [see, the right most panel of the middle row in fig. 6 of Patterson et al. (2002)] in the first week of the common superhump era, supports Lubow's theory because the excitation of the (2,3)-mode plays the most important role for the growth of the eccentric mode by the 3:1 resonance in his theory. The (2,3)-mode is two-armed spiral waves, rotating one and half times around the accretion disk over one superhump period in the inertial frame, as clearly seen in hydrodynamic simulations by Simpson and Wood (1998).

Another interesting aspect is a strong excitation of a mode with frequency ω_0, in particular, in the second week of the common superhump era of the 2001 outburst of WZ Sge. This is clearly seen in the lowest right panel of figure 7 by Patterson et al. (2002), and it was called the "orbital light curve" because it was obtained by synchronous summation at the orbital period. Patterson et al (2002) interpreted it as being a hot-spot light curve,

and they used it as evidence for enhanced mass transfer. This mode is a one-armed wave pattern with (1,1) fixed in the corotating frame of the binary, as discussed in the previous section.

In Lubow's theory for the excitation of eccentricity of a disk, it is a two-step process. In the first stage, the (1,0)-mode grows rapidly together with the (2,3)-mode launched by the 3:1 resonance. In the second stage, once the (1,0)-mode attains a large amplitude, various nonlinear wave couplings become important, and a kind of steady state is established between various wave modes. In this picture, the (1,1)-mode is also reinforced by nonlinear wave coupling between the original eccentric (1,0)-mode and the (0,1)-mode responsible for the superhump light variation. The (1,1)-mode observed with a large amplitude in the second week is thus a result of superhump phenomenon itself. If so, the amplitude of the (1,1)-mode will vary in a long run together with the amplitude of the (0,1)-mode; in other words, the amplitude of "orbital wave" in Patterson et al. (2001) should vary together with the superhump light amplitude, a picture already presented by Osaki and Meyer (2003).

6. Application to Other Systems

An SU UMa-type dwarf nova, IY UMa, is another eclipsing binary system for which Patterson et al. (2000) found a rich spectrum of frequencies in the power spectral analysis during its superoutburst. Its power spectrum is very similar to that of WZ Sge, because signals at $m\omega_0 - \Omega$ with $m = 3, 4, 5$ were found besides the well-known superhump periodicity at $\omega_0 - \Omega$. They are identified as $(m-1)$-armed traveling waves, just in the same way as in the case of WZ Sge, as discussed in sections 4 and 5.

There exist several eclipsing SU UMa stars. The most well known among them are OY Car, Z Cha, and HT Cas. Their superhump light curves could be examined by new light based on the concept of helical tomography.

The AM CVn stars are thought to be cataclysmic variable stars having helium-rich and hydrogen-deficient accretion disks (Warner 1995). In particular, its prototype star, AM CVn, itself exhibits very complex light variations. As already pointed out by Solheim and Provencal (1998), the disk structure will be analyzed by examining a rich spectrum of light curves of AM CVn stars. By analyzing its light curve, Skillman et al. (1999) have obtained periodic signals as many as 20 discrete frequencies. According to Skillman et al. (1999), the basic clocks of this star are an orbital period of 1028 s and a superhump period of 1051 s. However, many of the discovered frequencies can be understood as harmonics and sidebands of these fundamental frequencies, i.e., with $n\omega_0 - m\Omega$, where ω_0 and Ω are the orbital frequency and the apsidal precession frequency of an eccentric disk, respectively. On the other hand, Solheim et al. (1998) have made a quite different interpretation in that the fundamental frequency at 951μHz (with a period of 1051s) is related to the orbital period of the binary and the dominant light signal at 525 s is due to the two-armed spiral structure in the disk fixed in the corotating frame of the binary.

7. Summary and Discussions

We have proposed a new method to analyze complex superhump light curves of SU UMa stars with high orbital inclination, particularly for the 2001 outburst of WZ Sge. It is called the helical tomography because it can reconstruct a series of accretion disk images in various superhump phases. Based on the concept of helical tomography, power spectral data of superhump light curves obtained for the 2001 outburst of WZ Sge by Patterson et al. (2002) have been interpreted, and the azimuthal wave number of various frequency modes identified.

As already discussed in section 3, a very crude assumption had to be made for the superhump light distribution in order to perform an inversion of the orbital light curves into the azimuthal distributions of the superhump light. This is one of the biggest shortcomings in our theory and a much better method should be explored. Nevertheless, we can demonstrate that a two-armed traveling wave with $\cos(2\Theta - 3\omega_0 t)$ was excited vigorously in the first week of the common superhump era, supporting Lubow's (1991) theory of the eccentric Lindblad resonance for the tidal instability.

I would like to thank Dr. F. Meyer of Max-Planck-Institut für Astrophysik and Dr. M. Takata of The University of Tokyo for helpful discussions. This work is partly supported by a Grant-in Aid for Scientific Research No. 12640237 from the Ministry of Education, Culture, Sports, Science and Technology.

References

Hirose, M., & Osaki, Y. 1990, PASJ, 42, 135
Hirose, M., & Osaki, Y. 1993, PASJ, 45, 595
Ishioka, R., et al. 2002, A&A, 381, L41
Kato, T. 2002, PASJ, 54, L11
Lubow, S.H. 1991a, ApJ, 381, 259
Lubow, S.H. 1991b, ApJ, 381, 268
Murray, J. R. 1998, MNRAS, 297, 323
Osaki, Y., & Meyer, F. 2002, A&A, 383, 574
Osaki, Y., & Meyer, F. 2003, A&A, 401, 325
Patterson, J., Kemp, J., Jensen, L., Vanmunster, T., Skillman, D. R., Martin, B., Fried, R., & Thorstensen, J. R. 2000, PASP, 112, 1567
Patterson, J., et al. 2002, PASP, 114, 721
Simpson, J. C., & Wood, M. A. 1998, ApJ, 506, 360
Simpson, J. C., Wood, M. A., & Burke, C. 1998, Baltic Astron., 7, 255
Skillman, D. R., Patterson, J., Kemp, J., Harvey, D., Fried, R. E., Retter, A., Lipkin, Y., & Vanmunster, T. 1999, PASP, 111, 1281
Solheim, J.-E., et al., 1998, A&A, 332, 939
Solheim, J.-E., & Provencal, J. L. 1998, Baltic Astron., 7, 277
Warner, B., 1995, Ap&SS, 225, 249
Whitehurst, R. 1988, MNRAS, 232, 35